Journal of Southeast University (English Edition) Vol. 22, No. 1, pp. 59 – 63 Mar. 2006 ISSN 1003—7985

Novel gravity passive navigation system

Cai Tijing

(Department of Instrument Science and Technology, Southeast University, Nanjing 210096, China)

Abstract: According to the characteristics of gravity passive navigation, this paper presents a novel gravity passive navigation system (GPNS), which consists of the rate azimuth platform (RAP), gravity sensor, digitally stored gravity maps, depth sensor and relative log. The algorithm of rate azimuth platform inertial navigation system, error state-space equations, measurement equations and GPNS optimal filter are described. In view of the measurements made by an onboard gravity sensor the Eotvos effect is introduced in the gravity measurement equation of a GPNS optimal filter. A GPNS is studied with the Matlab/Simulink tools; simulation results demonstrate that a GPNS has small errors in platform attitude and position. Because the inertial navigation platform is the rate azimuth platform in the GPNS and gravity sensor is mounted on the rate azimuth platform, the cost of the GPNS is lower than existing GPNS's and according to the above results the GPNS meets the need to maintain accuracy navigation for underwater vehicles over long intervals.

Key words: gravity passive navigation system; rate azimuth platform; gravimeter; gravity map

When the significant development[1-6] of ultra-precise IMU based on cold atom interferometry makes the anomalous gravity vector be the most significant error source in the calculation of the navigation solution, the important gravity passive navigation technique has been paid more attention to by many countries in recent years. The effect of gravity compensation was investigated using direct interpolation and least square collocation[7]. A kriging algorithm[8,9] used to calculate the gravity field map was developed to localize a vehicle and bound navigational errors. In the 1990s, American Lockheed Martin Company developed a gravity passive navigation system[10,11], which included a universal gravity module, an inertial navigator module, a precision navigator module and a terrain estimation module. The universal gravity module contained a gravimeter and three gradiometers. The gravity passive navigation algorithm used gravity measurements, digitally stored gravity maps and navigator data to generate estimates of vehicle navigator errors. These estimates were then used to correct the inertial navigator on a continuous basis in order to bound navigation errors without the need for other external fixes. The GPNS was demonstrated during 1998 and 1999. The goal of this exercise shows that passive gravity navigation can hold the navigator error to less than 20% of the requirement[12]. Although the function and performance of American's GPNS are very strong, its price is very expensive. To make a navigation system have a passive function and lower its cost, a novel GPNS is proposed. The GPNS consists of gravity map and navigator with gravity measure, i.e., a rate azimuth platform with a highly precise gravity sensor. This paper presents the principle of a novel GPNS, the algorithm of a rate azimuth platform inertial navigation system (RAPINS), a GPNS extended Kalman filter and GPNS' simulation results.

Received 2005-07-04.

Biography: Cai Tijing (1961—), male, doctor, professor, caitij@seu.edu.cn.

1 Principle of GPNS

The GPNS consists of the rate azimuth platform, the gravity sensor, the relative log, the depth sensor, digitally stored gravity maps, computer and electronic circuitry. The rate azimuth platform is a two-ring type of platform composed of a gyrostabilizer and gimbals. Two sets of one-degree-freedom integrated gyros, a one-degree-freedom rate gyro and three single axis accelerometers are mounted on the gyrostabilizer. In the inner stabilization axis, a pitching torque motor and a pose angular sensor are placed on its two ends respectively. On the ends of outer stabilization axis, a rolling torque motor and a rolling pose sensor are arranged separately. Two integrated gyros and two accelerometers are used to measure and control the stabilization platform's turning, which makes the platform be parallel with the local horizontal level. The gravity sensor is also mounted on the gyrostabilizer and its sensed axis is perpendicular to the local horizontal level.

The block diagram of the GPNS implementation is shown in Fig. 1. The measured gravity at the true vehi-

cle position is the difference between the output of the gravity sensor and the Eotvos effect. The gravity derived from the gravity map at the navigator indicated that position could be calculated according to RAPINS offering position data. RAPINS indicated that navigation variables, the outputs of relative log and depth sensor, gravity map data and all above estimated variables were fed into the GPNS extended Kalman filter to get optimal estimates.

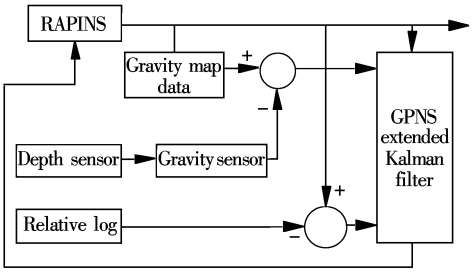

Fig. 1 Block diagram of GPNS implementation

2 RAPINS Algorithm

The definitions of coordinate frames are as follows: ① The local geodetic vertical (LGV) coordinate frame *OENU*. The origin is at the center of mass of the earth. The *ON* axis is in the direction of geodetic north; the *OE* axis is perpendicular to the meridian plane containing the vertical, directed toward the east; and the *OU* axis is directed outward along the local geodetic vertical. The geodetic vertical is everywhere normal to the reference ellipsoid. ② The local level coordinate frame $ox_ny_nz_n$. The oz_n axis is coincident with the *OU* axis, the ox_n axis and oy_n axis locate in the *OEN* plane and complete a right-handed system. In navigation process the local level coordinate frame rotates about the *OU* axis by an angular velocity $-\dot{K}$ with respect to the coordinate frame *OENU*. If the oy_n axis is coincident with the *ON* axis after calibration procedures, the azimuth angle of the local level coordinate frame is *K*, as shown in Fig. 2.

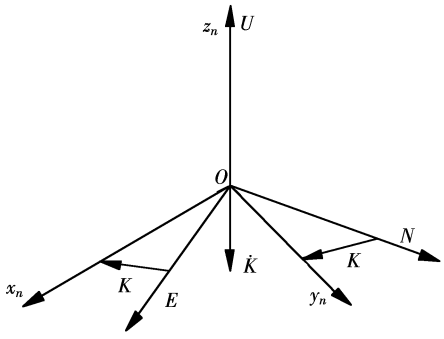

Fig. 2 Coordinate frames

The computed velocities and the geodetic longitude and latitude can be obtained as

$$V_{i,C}(t) = V_i(t_0) + \int_{t_0}^{t} a_{i,C}(\tau)\,d\tau \qquad i = E, N, U \tag{1}$$

$$\varphi_C(t) = \varphi(t_0) + \int_{t_0}^{t} \frac{V_{N,C}(\tau)}{R_\varphi(\tau)}d\tau \tag{2}$$

$$\lambda_C(t) = \lambda(t_0) + \int_{t_0}^{t} \frac{V_{E,C}(\tau)}{R_\lambda(\tau)\cos\varphi_C(\tau)}d\tau \tag{3}$$

$$K_C = K(t_0) + \int_{t_0}^{t} \left(-\omega_{U,0}(\tau) + \Omega\sin\varphi_C(\tau) + \frac{V_{E,C}(\tau)}{R_\lambda(\tau)}\tan\varphi_C(\tau) \right) d\tau \tag{4}$$

$$\begin{Bmatrix}\omega_x\\ \omega_y\end{Bmatrix} = \begin{bmatrix}\cos K_C & -\sin K_C\\ \sin K_C & \cos K_C\end{bmatrix}\begin{Bmatrix}\omega_{E,C}\\ \omega_{N,C}\end{Bmatrix} \tag{5}$$

where subscript C is used to designate the computed value; $a_{i,C}$ is the computed acceleration; $V_{E,C}$ and $V_{N,C}$ are the east and north computed velocities; R_φ and R_λ are the radii of curvature of the earth reference ellipsoid in north-south and east-west directions, respectively; λ is the geodetic longitude; φ is the geodetic latitude; $\omega_{U,0}$ is the practical output of rate azimuth gyro; Ω is the earth angular velocity; ω_x and ω_y are the platform commanded angular velocities, $\omega_{E,C} = -\dot{\varphi}_C$, $\omega_{N,C} = (\Omega + \dot{\lambda}_C)\cos\varphi_C$.

3 GPNS Extended Kalman Filter

The error equations of RAPINS can be expressed in state-space form as

$$\dot{\boldsymbol{X}}(t) = \boldsymbol{F}(t)\boldsymbol{X}(t) + \boldsymbol{G}(t)\boldsymbol{W}(t) \tag{6}$$

where $\boldsymbol{X}(t) = \{\phi_U, \phi_E, \phi_N, \Delta V_E, \Delta V_N, \Delta V_U, \Delta\varphi, \Delta\lambda, \Delta h, \varepsilon_x, \varepsilon_y, \varepsilon_z, \Delta A_x, \Delta A_y, \Delta A_z, \Delta Mg_x, \Delta Mg_y, \Delta Mg_z\}^T$; ϕ_E, ϕ_N and ϕ_U are the east, north and vertical attitude errors; ΔV_E, ΔV_N and ΔV_U are the errors in east, north and vertical velocities; $\Delta\varphi$, $\Delta\lambda$ and Δh are the errors in north latitude, east longitude and altitude; ε_x, ε_y and ε_z are the gyro bias drifts; ΔA_x, ΔA_y and ΔA_z are the accelerometer biases; ΔMg_x, ΔMg_y and ΔMg_z are the gyro scale factor errors; $\boldsymbol{F}(t)$ is the system dynamics matrix (18×18); $\boldsymbol{G}(t)$ is the input matrix (18×9); $\boldsymbol{W}(t)$ is the vector of white noise forcing functions (9×1). The elements of the system dynamics matrix $\boldsymbol{F}(t)$ are as follows:

$$f_{1,2} = \omega_N, \quad f_{1,3} = -\omega_E, \quad f_{1,4} = \frac{1}{R_E}\tan\varphi$$

$$f_{1,7} = \Omega\cos\varphi + \frac{V_E}{R_E\cos^2\varphi}$$

$$f_{1,10} = c_{31}, \quad f_{1,11} = c_{32}, \quad f_{1,12} = c_{33}$$

$$f_{1,16} = \omega_{xb}c_{31}, \quad f_{1,17} = \omega_{yb}c_{32}, \quad f_{1,18} = \omega_{zb}c_{33}$$

$$f_{2,1} = -\omega_N, \quad f_{2,3} = \omega_U, \quad f_{2,5} = -f_{7,5} = -\frac{1}{R_N}$$

$$f_{2,10}=f_{4,13}=c_{11},\quad f_{2,11}=f_{4,14}=c_{12},\quad f_{2,12}=f_{4,15}=c_{13}$$
$$f_{2,16}=\omega_{xb}c_{11},\quad f_{2,17}=\omega_{yb}c_{12},\quad f_{2,18}=\omega_{zb}c_{13}$$
$$f_{3,1}=\omega_E,\quad f_{3,2}=-\omega_U,\quad f_{3,4}=\frac{1}{R_E},\quad f_{3,7}=-\Omega\sin\varphi$$
$$f_{3,10}=f_{5,13}=c_{21},\quad f_{3,11}=f_{5,14}=c_{22},\quad f_{3,12}=f_{5,15}=c_{23}$$
$$f_{3,16}=\omega_{xb}c_{21},\quad f_{3,17}=\omega_{yb}c_{22},\quad f_{3,18}=\omega_{zb}c_{23}$$
$$f_{4,1}=a_N,\quad f_{4,3}=-a_U,\quad f_{4,4}=\frac{V_N\sin\varphi-V_U\cos\varphi}{R_E\cos\varphi}$$
$$f_{4,5}=(2\Omega+\dot{\lambda})\sin\varphi,\quad f_{4,6}=-(2\Omega+\dot{\lambda})\cos\varphi$$
$$f_{4,7}=V_U(2\Omega+\dot{\lambda})\sin\varphi+V_N(2\Omega+\dot{\lambda})\cos\varphi+\frac{V_E\sin\varphi}{R_E\cos^2\varphi}(V_N\sin\varphi-V_U\cos\varphi)$$
$$f_{5,1}=-a_E,\quad f_{5,2}=a_U$$
$$f_{5,4}=-(2\Omega+\dot{\lambda})\sin\varphi-\frac{V_E\sin\varphi}{R_E\cos\varphi},\quad f_{5,5}=-\frac{V_U}{R_N}$$
$$f_{5,6}=-\dot{\varphi},\quad f_{5,7}=-V_E(2\Omega+\dot{\lambda})\cos\varphi-\frac{V_E^2\sin^2\varphi}{R_E\cos^2\varphi}$$
$$f_{6,2}=-a_N,\quad f_{6,3}=a_E$$
$$f_{6,4}=(2\Omega+\dot{\lambda})\cos\varphi+\frac{V_E}{R_E},\quad f_{6,5}=2\dot{\varphi}$$
$$f_{6,7}=-V_E(2\Omega+\dot{\lambda})\sin\varphi+\frac{V_E^2\sin\varphi}{R_E\cos\varphi}$$
$$f_{6,13}=c_{31},\quad f_{6,14}=c_{32},\quad f_{6,15}=c_{33}$$
$$f_{8,4}=\frac{1}{R_E\cos\varphi},\quad f_{8,7}=\frac{V_E\sin\varphi}{R_E\cos^2\varphi},\quad f_{9,6}=1$$

where $c_{ij}(i,j=1,2,3)$ are the elements of the transformation matrix from local level coordinate frame to the LGV coordinate frame, $a_i(i=E,N,U)$ are the projections of specific force on the LGV coordinate frame, and $\omega_{ib}(i=x,y,z)$ are the projections of angular velocities on the local level coordinate frame.

The discrete measurement equations of relative log can be expressed as

$$z_{V_E^L}(t_{k+1})=\Delta V_E(t_{k+1})-V_N\phi_U-V_{TE}(t_{k+1})-\nu_{V_E}(t_{k+1}) \tag{7}$$

$$z_{V_N^L}(t_{k+1})=\Delta V_N(t_{k+1})+V_E\phi_U-V_{TN}(t_{k+1})-\nu_{V_N}(t_{k+1}) \tag{8}$$

where V_{TE} and V_{TN} are the east and north sea-flow velocities; ν_{V_E} and ν_{V_N} are the measurement noises in east and north sea-flows.

The measurement equation of the gravity sensor is

$$Z_g=g(\tilde{\varphi},\tilde{\lambda})-(\tilde{g}(\varphi,\lambda)+E_C)=(g(\tilde{\varphi},\tilde{\lambda})-g(\varphi,\lambda))-(E_C-E)=\frac{\partial g}{\partial\varphi}\Delta\varphi+\frac{\partial g}{\partial\lambda}\Delta\lambda-\left(\frac{\partial E}{\partial V_E}\Delta V_E+\frac{\partial E}{\partial V_N}\Delta V_N+\frac{\partial E}{\partial\varphi}\Delta\varphi\right)+\nu_g \tag{9}$$

where $g(\tilde{\varphi},\tilde{\lambda})$ is the gravity derived from the map at the navigator indicated position $(\tilde{\varphi},\tilde{\lambda})$, $\tilde{g}(\varphi,\lambda)$ is the gravity sensor output, $g(\varphi,\lambda)$ is the measured gravity at the true vehicle position (φ,λ), $E=2\Omega V_E\cos\varphi+(V_E^2+V_N^2)/R$ is the Eotvos effect, E_C is the computed value of Eotvos effect, and ν_g is the sum of gravity sensor noise and gravity map error. It is noticeable that before gravity map matching the measured gravity at the true vehicle position is not known in advance. When vehicle exercises, RAPINS moves relative to the earth and produces centripetal and the Coriolis accelerations. The vertical component of these accelerations affects measured gravity; therefore, the Eotvos effect must be contained in the measurement equation of the gravity sensor. The gravity gradients are determined by the gravity map.

The discrete linearized GPNS extended Kalman filter can be described as

$$\boldsymbol{x}_{k+1}=\boldsymbol{\Phi}_{k+1/k}\cdot\boldsymbol{x}_k+\boldsymbol{\Gamma}_{k+1/k}\cdot\boldsymbol{w}_k \tag{10}$$
$$\boldsymbol{z}_{k+1}=\boldsymbol{H}_{k+1}\cdot\boldsymbol{x}_{k+1}+\boldsymbol{\nu}_{k+1} \tag{11}$$

where $\boldsymbol{x}_k=\boldsymbol{x}(t_k)=\{\phi_U,\phi_E,\phi_N,\Delta V_E,\Delta V_N,\Delta V_U,\Delta\varphi,\Delta\lambda,\Delta h,\varepsilon_x,\varepsilon_y,\varepsilon_z,\Delta A_x,\Delta A_y,\Delta A_z,\Delta Mg_x,\Delta Mg_y,\Delta Mg_z,V_{TE},V_{TN}\}^{\mathrm{T}}$, $\boldsymbol{\Phi}_{k+1/k}\cong\boldsymbol{E}_{n\times n}+\boldsymbol{F}(t_k)\cdot\Delta T+\frac{1}{2}[\boldsymbol{F}(t_k)\cdot\Delta T]^2$, $\boldsymbol{\Gamma}_{k+1/k}\cong\boldsymbol{\Phi}_{k+1/k}\cdot\boldsymbol{G}(t_k)\cdot\Delta T$.

The algorithm of the GPNS extended Kalman filter in closed-loop form is as follows:

$$\tilde{\boldsymbol{x}}_{k+1}=\boldsymbol{K}_{k+1}\boldsymbol{Z}_{k+1} \tag{12}$$
$$\boldsymbol{P}_{k+1/k}=\boldsymbol{\Phi}_{k+1/k}\boldsymbol{P}_k\boldsymbol{\Phi}_{k+1/k}^{\mathrm{T}}+\boldsymbol{\Gamma}_{k+1/k}\boldsymbol{Q}_k\boldsymbol{\Gamma}_{k+1/k}^{\mathrm{T}} \tag{13}$$
$$\boldsymbol{K}_{k+1}=\boldsymbol{P}_{k+1/k}\boldsymbol{H}_{k+1}^{\mathrm{T}}(\boldsymbol{H}_{k+1}\boldsymbol{P}_{k+1/k}\boldsymbol{H}_{k+1}^{\mathrm{T}}+\boldsymbol{R}_{k+1})^{-1} \tag{14}$$
$$\boldsymbol{P}_{k+1}=(\boldsymbol{E}_{n\times n}-\boldsymbol{K}_{k+1}\boldsymbol{H}_{k+1})\boldsymbol{P}_{k+1/k} \tag{15}$$

where $\boldsymbol{Q}_{k+1}=\frac{\boldsymbol{Q}(t_{k+1})}{\Delta T}$ is the covariance matrix of input white noise forcing functions, and $\boldsymbol{R}_{k+1}=\frac{\boldsymbol{R}(t_{k+1})}{\Delta T}$ is the covariance matrix of measurement white noise.

4 Simulation Results

The computational simulation of the GPNS was carried out by the Matlab/Simulink tools. The resolution of the gravity map is 0.005°. The vehicle with the GPNS has initial conditions and model parameters as follows: $V_N=15$ m/s, $V_E=0$, $\phi_x(0)=45''$, $\phi_y(0)=45''$, $\phi_U(0)=2'$, $\Delta V_E(0)=0.3$ m/s, $\Delta V_N(0)=0.3$ m/s, $\Delta V_U(0)=0.3$ m/s, $\Delta\varphi(0)=5''$, $\Delta\lambda(0)=5''$, $\Delta h(0)=1.0$ m, $\varepsilon_x(0)=\varepsilon_y(0)=0.01$ (°)/h, $\varepsilon_z(0)=0.05$ (°)/h, $\Delta A_x=\Delta A_y=\Delta A_z=5\times10^{-5}g$, $\Delta M_{gx}=\Delta M_{gy}=\Delta M_{gz}=0.3\%$, $\Delta V_{TE}=\Delta V_{TN}=0.02$ m/s, inertial error covariance matrix $\boldsymbol{P}(0)=2\times\mathrm{diag}\{X_i(0)^2\}$, $i=1,2,\ldots,20$, the filter period is 60 s. Fig. 3 shows the variability of attitude error angles of the GPNS with time. The pitch and roll error angles are less than 18″(RMS), the azimuth error angle is less

than 1′(RMS). The curves of latitude and longitude errors of the GPNS as a percent of goal are plotted in Fig. 4. The position error is less than 15% (RMS) of goal. If the GPNS is used with no gravity map, the position errors increase with time. Fig. 5 shows the variability of latitude and longitude errors of RAPINS with velocity damping with time. RAPINS position and attitudes errors with time were described in Ref. [13].

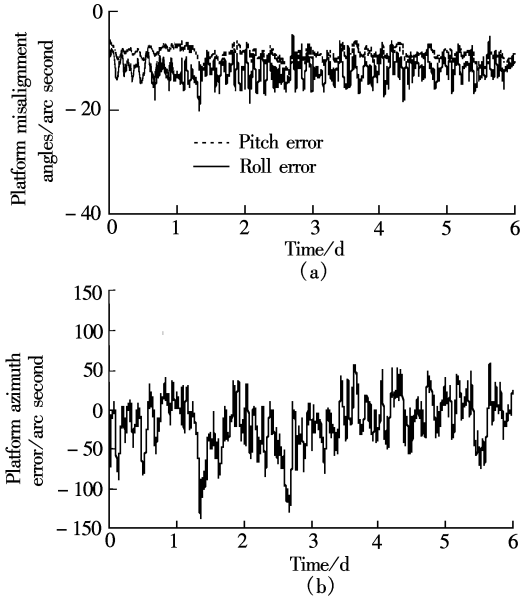

Fig. 3 Variability of attitude error angles of GPNS with time. (a) Pitch error and roll error; (b) Azimuth error

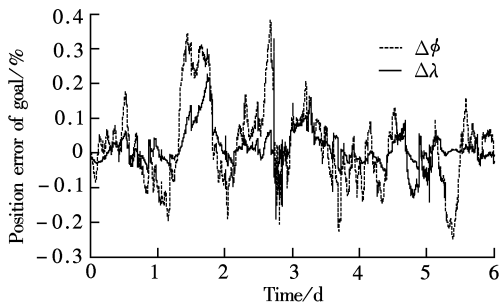

Fig. 4 Latitude and longitude errors of GPNS

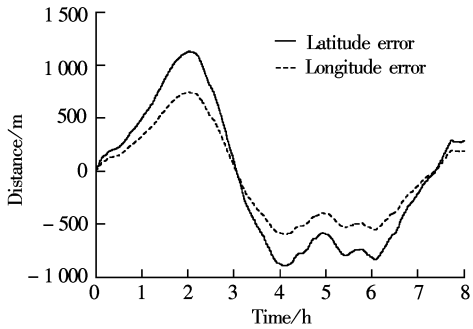

Fig. 5 Latitude and longitude errors of RAPINS

5 Conclusion

A technique has been presented that utilizes rate azimuth platform, gravity sensor, gravity maps, depth gauge and relative log to passively bound inertial navigation system position error. Simulation results indicate that position-bounding goal is being met. The GPNS not only has low costs, but also is able to meet requirements to maintain high accuracy navigation for underwater vehicles over long intervals.

References

[1] Kasevich M A. Coherence with atoms [J]. *Science*, 2002, **298**(5597): 1363 − 1368.

[2] McGuirk J M, Foster G T, Fixler J B, et al. Sensitive absolute-gravity gradiometry using atom interferometry [J]. *Phys Rev A*, 2002, **65**(3B): 033608/01 − 033608/14.

[3] Peters A, Chung K Y, Chu S. High-precision gravity measurements using atom interferometry [J]. *Metrologia*, 2001, **38**(1): 25 − 61.

[4] Gustavson T L, Landragin A, Kasevich M A. Rotation sensing with a dual atom interferometer Sagnac gyroscope [J]. *Class Quantum Grav*, 2000, **17**(12): 2385 − 2398.

[5] Jekeli C. Cold atom interferometer as inertial measurement unit for precision navigation[C]//*Proceedings of the Annual Meeting-Institute of Navigation*, 60*th Annual Meeting of the Institute of Navigation*. Dayton, OH, USA, 2004: 604 − 613.

[6] Durfee D, Fixler J, Foster G. Atom interferometer inertial force sensors[C]//*IEEE* 2000 *Position Location and Navigation Symposium*. Piscataway: IEEE Inc, 2000: 395 − 398.

[7] Kwon Jay H. Gravity compensation methods for precision INS[C]//*Proceedings of the Annual Meeting-Institute of Navigation*, 60*th Annual Meeting of the Institute of Navigation*[C]. Dayton, OH, USA, 2004: 483 − 490.

[8] Carner C B. Gravitational field maps and navigational errors[J]. *IEEE Journal of Oceanic Engineering*, 2002, **27**(3): 726 − 737.

[9] Kamger-Parsi B, Kamger-Parsi B. Vehicle localization of gravity maps [C]//*Proc SPIE Conf Unmanned Vehicle Technology*. Orlando, FL, USA, 1999: 182 − 191.

[10] Lowrey J A Ⅲ, Shellenbarger J C. Passive navigation using inertial navigation sensors and maps [J]. *Naval Engineers Journal*, 1997, **109**(3): 245 − 251.

[11] Moryl J. Advanced submarine navigation systems [J]. *Sea Technology*, 1996, **37**(11): 33 − 39.

[12] Rice Hugh, Mendelsohn Louis, Aarons Robert, et al. Next generation marine precision navigation system [C]//*IEEE* 2000 *Position Location and Navigation Symposium*. New York: IEEE Inc, 2000: 200 − 206.

[13] Cai Tijing, Emeliantsev G I. Study on the rate azimuth platform inertial navigation system [J]. *Journal of Southeast University*: *English Edition*, 2005, **21**(2): 29 − 32.

新型的重力无源导航系统

蔡体菁

(东南大学仪器科学与工程系,南京 210096)

摘要:针对重力无源导航的特点,提出了一种由速率方位惯性平台、重力传感器、重力图、深度计和相对计程仪组成的新型重力无源导航系统,给出了速率方位惯性平台系统的导航算法、重力无源导航系统的最优滤波器、误差状态方程和测量方程.考虑到运动载体上重力传感器的输出特性,在最优滤波器的重力观测方程中引入了厄特弗斯效应.应用 Matlab/Simulink 工具对此重力无源导航系统进行了计算机仿真研究,仿真结果表明此重力无源导航系统的平台姿态角误差和定位误差小,能够满足水下运载体长期高精度导航的要求.又由于本系统采用了速率方位惯性平台,且把重力敏感器置于其上,省去了重力仪,所以与现有的重力无源导航系统相比成本较低.

关键词:重力无源导航系统;速率方位平台;重力仪;重力图

中图分类号:TN967.2